




Research Article

Movement tracing and analysis of benthic sting ray (*Dasyatis akajei*) and electric ray (*Narke japonica*) toward seabed exploration



Shun-ichi Funano¹ · Nobuyuki Tanaka¹ · Satoshi Amaya¹ · Akira Hamano² · Toyoki Sasakura³ · Yo Tanaka¹ 

Received: 19 August 2020 / Accepted: 25 November 2020 / Published online: 9 December 2020
© The Author(s) 2020 

Abstract

Creation of a seabed map is a significant task for various activities including safe navigation of vessels, commercial fishing and securing sea-mined resources. Conventionally, search machines including autonomous underwater vehicles or sonar systems have been used for this purpose. Here, we propose a completely different approach to improve the seabed map by using benthic (sting and electric) rays as agents which may explore the seabed by their autonomous behavior without precise control and possibly add extra information such as biota. For the first step to realize this concept, the detail behavior of the benthic rays must be analyzed. In this study, we used a system with a large water tank (10 m × 5 m × 6 m height) to measure the movement patterns of the benthic rays. We confirmed that it was feasible to optically trace the 2D and 3D movement of a sting and an electric ray and that the speed of the rays indicated whether they were skimming slowly over the bottom surface or swimming. Then, we investigated feasibility for measuring the sea bottom features using two electric rays equipped with small pingers (acoustic transmitters) and receivers on a boat. We confirmed tracing of the movements of the rays over the sea bottom for more than 90 min at 1 s time resolution. Since we can know whether rays are skimming slowly over the bottom surface or swimming in water from the speed, this would be applicable to mapping the sea bottom depth. This is the first step to investigate the feasibility of mapping the seabed using a benthic creature.

Keywords Benthic ray · Electric ray · Sting ray · Seabed mapping

1 Introduction

In the past few decades, there have been increasing demands for seabed mapping [1, 2]. Seabed maps are important for safe navigation of vessels, securing natural resources including fossil fuels and minerals and undertaking better commercial fishery activities. The use of autonomous underwater vehicles (AUVs) is one common

method for seabed searching [3–6]. AUVs are convenient tools for getting the shape of the sea bottom in detail. Alternatively, sonar systems have been used for this purpose [7–9]. These use acoustic remote sensing from ships and are very powerful tools to search the sea bottom even at great depths. Multibeam echosounders (MBES) are currently the main devices which are used for high-resolution seabed mapping [10–13]. Optical methods using

Shun-ichi Funano and Yo Tanaka have contributed equally to this work.

Electronic supplementary material The online version of this article (<https://doi.org/10.1007/s42452-020-03967-6>) contains supplementary material, which is available to authorized users.

✉ Yo Tanaka, yo.tanaka@riken.jp | ¹Center for Biosystems Dynamics Research (BDR), RIKEN, 1-3 Yamadaoka, Suita, Osaka 565-0871, Japan. ²National Fisheries University, 2-7-1 Nagata-Honmachi, Shimonoseki, Yamaguchi 759-6595, Japan. ³AquaSound Inc, 4-1-1 Minatojima Nakamachi, Chuo-ku, Kobe, Hyogo 650-0046, Japan.



SN Applied Sciences (2020) 2:2142 | <https://doi.org/10.1007/s42452-020-03967-6>

satellites [14–16] or laser scanning [17] are also candidates for searching tools. These optical methods can scan large areas without using ships or robots to actually visit the sites if the depth is within 10 m.

Although these methods are well established and promising to create a seabed map in large areas, we here propose a completely new approach to further improve the map. Our concept is to use benthic creatures as an agent for seabed exploration. A seabed map may be created by tracing the position of the autonomously moving creature (Fig. 1a). Moreover, benthic creatures have some level of intelligence in addition to their benthic property. Therefore, they can be utilized to obtain not only topographic information but also information about biota including feed or natural enemies present in an area in the future.

In this method, a small communication device (slave unit) is attached to the benthic creature, and the slave unit periodically sends a position signal to a receiver (master unit). Considering the need for an electrical source for long-term tracing, we consider that the electrical energy should be secured from the creature. Then, we selected an electric ray as the best option among various benthic creatures. Electric rays are found in all tropical to temperate waters worldwide [18], and they are known to produce a

strong electrical current to capture prey or to escape from enemies [19, 20]. We have previously developed an electric generator using electric organs of an electric ray driven by adenosine triphosphate (ATP) [21]. In this previous study, we also measured power generation of individual electric rays and found that a strong pulse-type electrical power of over 100 W was produced. This would be enough to drive a communication device. There are no other creatures in the sea that have such a strong electrical power as electric rays.

As a communication device, an ultrasonic transmitter called a pinger is used to trace the movement of fish [22]. Recently, pinger sizes have become very small, under 3.6 cm [23, 24], and that allows them to be attached onto small fish. For a moving electric ray that has a pinger attached onto it, by receiving the signal at multiple points, the position of the ray can be estimated (Fig. 1b) [25]. It is known that electric rays are generally considered as benthic [26], but detailed observations that trace their actual movement behavior in the sea have not been reported. It is indispensable to know the detail behavior of electric rays for creating a map by plotting 3D motion in a clearly known topography in a precise manner and validate whether the observed motion can be utilized for seabed mapping.

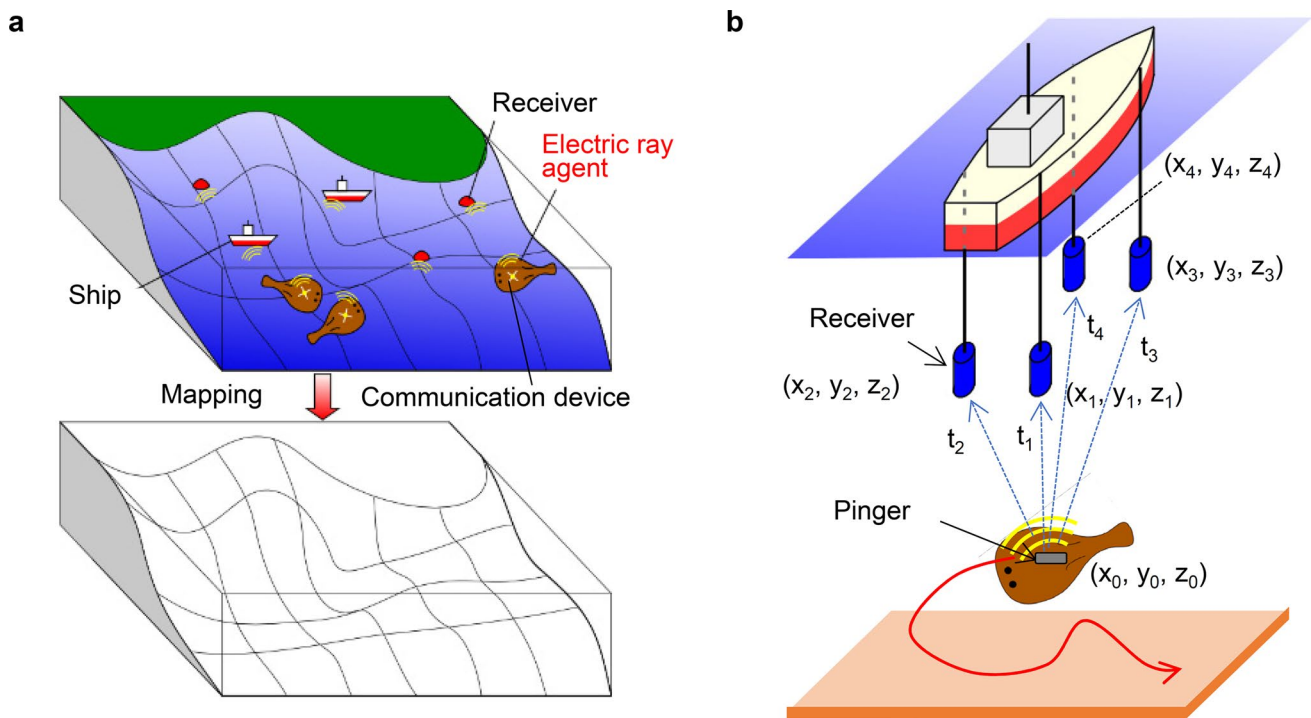


Fig. 1 Concept of this study. **a** A method for seabed mapping using an electric ray agent. **b** Measurement principle for determining the position of the agent using a pinger. Parameters x_0, y_0 and z_0 denote the position of the agent, while x_i, y_i and z_i are the posi-

tion of the receiver ($i=1, 2, 3, \dots$). The position of the agent can be calculated from the positions of the receivers and communication time, t_i ($i=1, 2, 3, \dots$) when i is 3 (the number of parameters: x_0, y_0 and z_0) or over

Based on this concept, our aim in this study was to optically measure the 3D motion of electric rays using a large water tank with transparent windows, followed by the actual measurement in the open sea of 3D trajectories of electric rays by acoustic tracing using a pinger installed on the rays.

In this study, before carrying out the experiments using electric rays, we used sting rays due to the following reason. Although sting rays do not generate electricity, they are similar in size with electric rays and also known as benthic rays [27]. More importantly, sting rays can be obtained in the summer which is just opposite to the electric rays which can be often obtained in the winter statistically. This fact means that the limitation of research period could be overcome by using sting rays. Although electric rays are favorable because they have electricity, the final goal is to use similar benthic creatures like sting rays if energy harvesting methods can be developed. In such a viewpoint, it is important to confirm that sting rays can be also used as agents for seabed mapping for future experimental convenience toward creature-based exploration in a large area. Another purpose of this experiment was to confirm that the large water tank and video cameras are useful for tracking the movement of fish with satisfactory resolution.

2 Materials and methods

2.1 Ethical approval

All animal experiments were approved by the Animal Care and Experimentation Committee of RIKEN (Institute of Physical and Chemical Research, Japan) and were carried out in accordance with the approved guidelines. The underwater weight of the small camera and pinger was less than 5% of the weight of the rays used.

2.2 The water tank

The water tank used for the experiments was located at the Hakodate Research Center for Fisheries and Oceans, Hokkaido, Japan. This water tank had front and back lengths of 10 m each, 5 m side length, and 6 m height. Because the bottom of the water tank was slimy, it was washed and dried before being prepared for the preliminary experiments. Retroreflective yellow tapes (RF30Y50, DIATEX, Tokyo, Japan) were affixed parallel to the side walls at intervals of 2.5 m on the bottom of the water tank. Two nets with a length of 5 m, a height of 2.5 m, and 3-cm square mesh (Nihon Matai, Tokyo, Japan) were used for partitioning of the water tank and limiting the movement space of the sting and electric rays. The tank was partitioned to make rays be in the area where cameras

can trace. Six aluminum pipes as weights were attached using cable ties to the lower end of each net at equal intervals. Four styrofoam floats were attached with cable ties to the top of each net at equal intervals. Two suction cups were attached to the ends of each net for attachment to the water tank walls. The nets were installed at positions 2.5 m from the left and right sides of the water tank (this placed the nets above 2 of the yellow tapes). Weights were attached to a plastic plate (70 cm width, 2 m height), a desk (45 cm width, 80 cm depth, 75 cm height) and a seaweed bed (50 cm × 40 cm). These objects were placed in the water tank to imitate the seabed. After this, the water tank was filled to a depth of 2.3 m. We did not use natural seafloor. This is because we focused on tracing the behavior by the video image. If rays were hidden under sediment, it would be difficult.

2.3 Setup of video cameras

We set video cameras as follows. Video cameras (HDR-PJ800 and HDR-CX485, Sony, Tokyo, Japan) were attached to tripods and were placed at the front, on the left side of the tank as viewed from the front, and at the top of the water tank. The camera height was adjusted to 1.5 m on the tripods. The area around the water tank was covered with a black curtain to block out ambient light. The video resolution and frame rate were 1280 × 720 pixels and 30 frames per second, respectively. The video data for more than 8 h were recorded on SD cards (128 GB).

2.4 The sting rays and electric rays

Sting rays (*Dasyatis akajei*) and electric rays (*Narke japonica*) were obtained from Aquamarinzu (a fishing company located in Minamiise, Mie, Japan). For the preliminary water tank experiments, two sting rays (one was for tracing experiment and another was for water-resistant video camera experiment) were sent to the research center three weeks before the experiment day and electric rays were sent to the research center 1 and 2 weeks before the experiment day (this difference was due to the experimental schedule). They were stored in a small water tank. The weights of the sting and the electric rays used for water tank experiments were 80 g and 300 g, respectively. For transfer to the large water tank, the sting ray or the electric ray was put into a bucket and lowered from above to the water surface. In the seabed research experiment, electric rays were sent to the experimental site the day before the experiment day. The weights of the 2 electric rays used in the seabed experiment were 400 g and 300 g, respectively. The rays were connected by a fishing line with a hook from their mouth to a fishing rod on the fishing boat not to let the rays escape from the measurement area.

2.5 Setup for 2D movement analysis using a sting ray

In this experiment, just one video camera was used to get a view from the top toward the tank bottom (Fig. 2a); this placed the experimental attention on the movement track measurement in the X–Y plane. Various items were set up in the empty tank. To visualize the coordinates, yellow tapes were pasted on the tank bottom (Fig. 2b). The center of the bottom (crossing point of the tapes) was defined as the zero point ($x=y=0$). Nets were put along both sides of the measurement area (the central part of the tank) from the bottom to a height of 3 m (the water depth was also 3 m) so as not to miss the ray. Additionally, a plastic plate, a seaweed bed and a desk were placed on the bottom in order to confirm that the place which cannot be seen from the top could be observed by the video camera equipped with the ray. Photographs of the water tank and the setup in the tank are shown in Fig. 2c, d, respectively. Finally, the tank was filled with seawater to be a height of 3 m, and then, the sting ray was put into the center of the tank. The ray swam about and then went to the bottom within a few minutes.

2.6 Installing a water-resistant video camera on a ray

For the additional experiment, a small water-resistant video camera (Quelima SQ12, China) was attached to the upper surface of a sting ray body, in order to record underwater video as follows. The outer edge of a security tag (Digisto, Oita, Japan) was cut off. The security tag was attached to a waterproof case for the camera using glue (AR-R30, NICHIBAN, Tokyo, Japan). The camera was put in the waterproof case. The underwater weight of the waterproof case with the small camera was under 4 g. The waterproof case was attached to a sting ray or electric ray with a pin paired with the security tag. The pin was stabbed into the edge muscle of the ray body. The video resolution and frame rate were 1280×720 pixels and 30 frames per second, respectively. The video data were recorded on SD cards (32 GB). The ray was then put into the center of the tank.

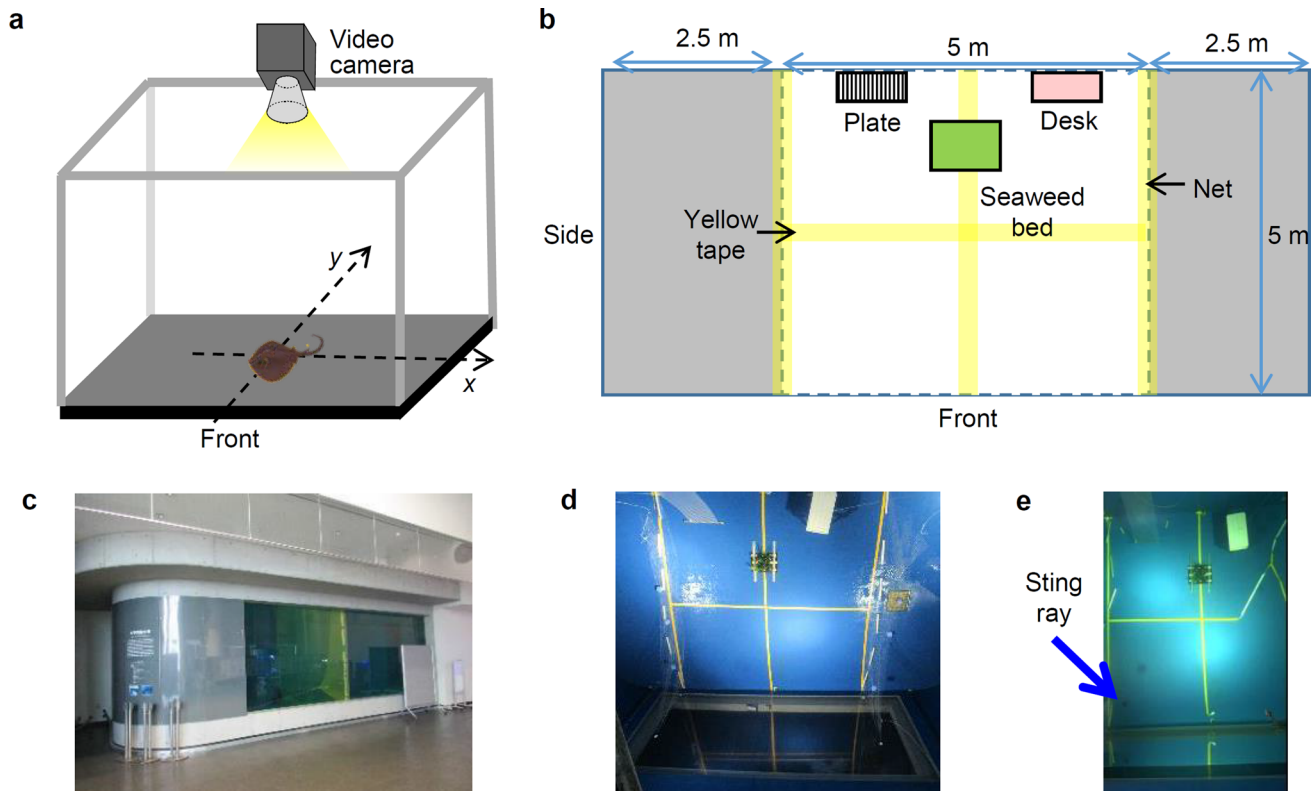


Fig. 2 Setup for measurement of the 2D movement of a sting ray in a water tank. **a** Measurement using a video camera at the top of the tank, and the definition of the coordinates in this measurement. **b** Setup showing objects on the bottom of the water tank and the

tank dimensions. **c** A photograph of the water tank from the front direction. **d** A photograph of the bottom of the water tank with the objects in place. **e** A photograph of the bottom of the water tank after the ray was put into the tank

2.7 Coordinate calibration

In the 3D movement analysis experiment using an electric ray, the distortion of the image increases with the distance from the center because of the characteristics of the camera lens. It is necessary to correct the length because the apparent length and the actual length differ especially in the y -axis direction which is the horizontal direction of the image with more pixels than the vertical direction. The length from the vertical line to the wall is 2.5 m. However, the apparent 2.5 m is gradually lengthened from the bottom of the water tank to the surface of the water due to distortion of the video camera lens. Therefore, Eq. (1) was formulated to calculate the y -axis value from the z -axis value of the electric ray:

$$y = \left(\frac{2.5y'}{az + b} \right) \quad (1)$$

where y' is the number of pixels from the vertical line to the ray, z is z -axis value (m), a is the gradient (of the line connecting y position of the wall at $z=0$ and 2.5) [a constant], and b is the intercept (y' value when $z=0$) [a constant].

The denominator on the right side of Eq. (1) indicates the number of pixels for $y=2.5$ m at arbitrary height. The y -axis values were calculated by Eq. (1) in this experiment.

2.8 Installing pinger on a ray

We attached a pinger to a ray to obtain the position as follows. The outer edge of a security tag was cut off. The security tag was attached to a pinger (AQPX-1030P, Aqua-Sound, Kobe, Japan) with glue. After the glue was cured, the pinger and tag were wrapped in thread seal tape (polytetrafluoroethylene (PTFE) film tape; NITOFロン Pipe Seal, Nitto Denko, Osaka, Japan) for reinforcement. The underwater weight of the pinger with the security tag was 1.6 g. The pinger with the security tag was attached to each electric ray with a pin paired with the security tag. The pin was stabbed into the edge muscle of the ray body. The operating conditions of the pingers were as follows: sound wave frequency, 62.5 kHz; transmission cycle, 1 s; sound pressure level, 155 dB re 1 μ Pa at 1 m; identification codes, 8, 9 and 10 (electric ray #1, #2 and control, respectively); and battery life, at least 2 days (transmission cycle, 1 s).

2.9 Image analysis

The acquired video images were analyzed by using movie editing software (PowerDirector 16, CyberLink, New Taipei, Taiwan; Kinovea, <https://www.kinovea.org/>).

Every frame was captured and pasted into drawing software. The values were calculated with spreadsheet software (Excel 2013, Microsoft, WA, USA).

3 Results

3.1 2D movement analysis using a sting ray

Before carrying out the experiments using electric rays, we used sting rays (*Dasyatis akajei*) by the reason described in Introduction.

The movement of the sting ray is shown in Fig. 3a as frames captured from Supplementary Movie S1. The movement trajectory is drawn in the X - Y coordinates in Fig. 3b. The displacement time-course trajectory for the sting ray as directly observed from the recorded video is plotted in Fig. 3c. Although the movement was very slow (2 m/h in maximum from Fig. 3c), we confirmed that the ray moved along the bottom and near the corners where the nets were attached to the water tank walls. The ray was alive and unharmed after 8 h of the observation. The observations showed that the sting ray mostly moved along the bottom of the tank. From these results, we guessed that sting rays can be used as agents for obtaining geometric information by position notification using a communication device and thus can be substituted for electric rays in the summer if using batteries for the communication device instead of autologous electricity. Here, assumed batteries are the same one equipped with pingers which were used for electric ray experiments in the sea, which are described in Sect. 2.8. Also, we found that the movement of the ray could be plotted by this method with centimeter resolution (0.7 cm) using a camera located as much as 6 m away from the tank bottom.

In order to verify that a sting ray can also be used for obtaining video images, a small water-resistant video camera was attached and put into the center of the tank. After reaching the bottom of the tank, the ray swam in circles at the bottom, and the camera caught views at all angles of the bottom of the tank, including underneath the metal plate and other obstacles which cannot be seen from the top, as shown in Supplementary Fig. S1 and Supplementary Movie S2. Movements of the ray were observed for at least 30 min, and then, the ray was caught and checked to be unharmed. This result indicated that the benthic ray could be used for obtaining the water bottom images from a camera directly attached on the ray. To realize this concept, the transfer technology for big size data must be developed as a future perspective.

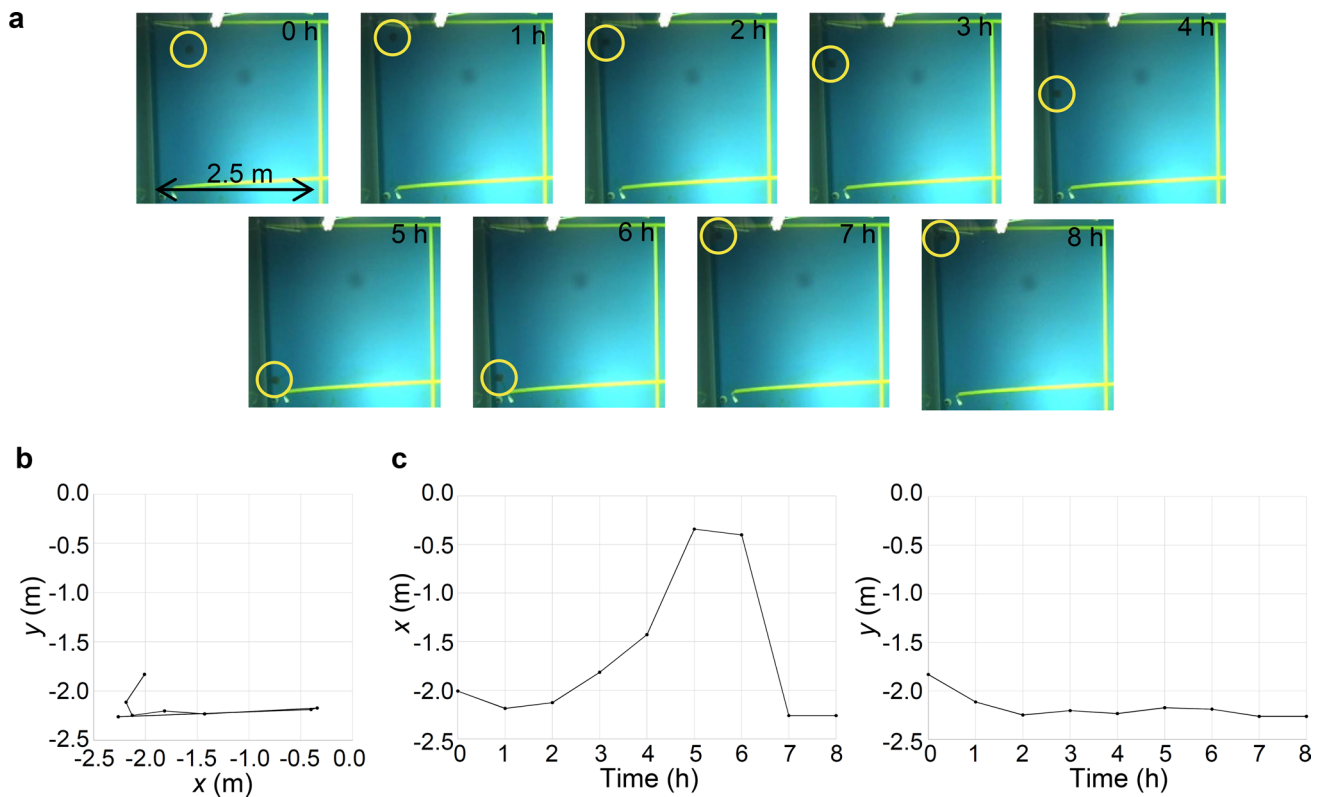


Fig. 3 Measurement result of the 2D movement of a sting ray in a water tank. **a** Sequential video frames showing the movement of the sting ray. Circles indicate the ray. **b** Graph plotting the move-

ment of the ray on the X–Y plane during 1 h. **c** Time courses of the movement of x and y values of the ray

3.2 3D movement analysis using an electric ray

Based on the results above, in the third-type experiment using the same water tank, we tried to track the 3D movement of electric rays (Fig. 4a). Yellow tapes and nets were set in the water tank as described for the first two experiments. However, obstacles were not set (Fig. 4b). Acoustic methods to track the electric ray (described in the next section) were not used because reflections by the tank walls would disturb the acoustic signal. Instead, we acquired images from 3 directions, and the 3D coordinate values were defined by correction of the raw image data. The center of the bottom (crossing point of the tapes) was defined as the zero point ($x=y=z=0$).

An electric ray (*Narke japonica*) was introduced into the water tank, and its movements were observed for about 30 min. This was shorter than the observation time for the sting ray because the electric ray moved faster than the sting ray did. Raw movie data are shown in Supplementary Movie S3. Images from each direction while the electric ray was stationary at the bottom are shown in Fig. 4c. From the movie data, it was clear that the ray was initially swimming but soon went to the bottom. After that, it was stationary for a while and then moved to another place and became

stationary there. This movie indicated that the electric ray actually spent most of its time along the tank bottom. We judged it would be possible to guess whether the ray was swimming or stationary on the bottom using the speed of the ray.

The trajectories of the electric ray were made from the movie data as follows. Time synchronized images from each direction are obtained from Supplementary Movie S3. When the electric ray was swimming, most of that time it was on the far side from the front as seen from the movie. Therefore, the z-axis values were measured with reference to the bottom surface in the left panel of Fig. 4c without correction. The relationship between the obtained z-axis values and time t was plotted (Fig. 5c (right)). The middle panel of Fig. 4c was used to measure the x- and y-axis values. Because of the characteristics of the camera lens and the actual distance from the center line, y-axis values were calibrated to correct the distortion of the images as described in Sect. 2.7. The relationship between the obtained y-axis values and time t was plotted (Fig. 5c (middle)). On the other hand, the distortion in the vertical direction was not so large because the aspect ratio (the ratio of width to height) of the image was 16:9. In addition, when the electric ray was swimming, it was generally near

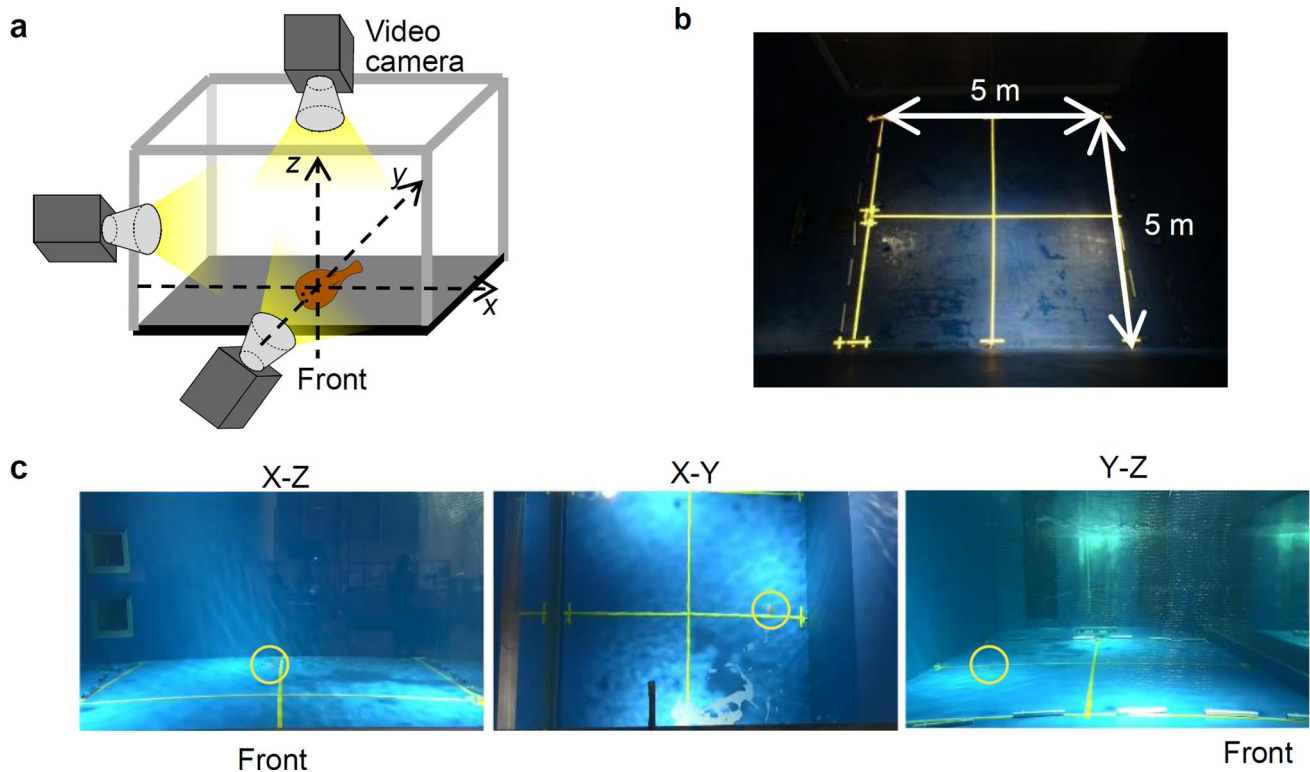


Fig. 4 Setup for the measurement of the 3D movement of an electric ray in a water tank. **a** Measurement method using 3 video cameras (top, front, side), and the definition of the coordinates in this measurement. **b** A photograph of the water tank from the front

direction. **c** Photographs of the water tank from the top, front and side directions after putting the ray into the tank. Circles indicate the ray

the horizontal line ($x=0$). Therefore, the x -axis values were measured without correction. The relationship between the obtained x -axis values and time t was plotted (Fig. 5c (left)). Figure 5a and b is made from connecting the x -, y -, and z -axis values in each t point obtained above. In this experiment, the right panel of Fig. 4c was not used to make the position coordinates of the electric ray. This was because the movement in the y -axis direction was not so large when the electric ray was swimming. If the electric ray had a different trajectory, the right panel of Fig. 4c might have been used.

The trajectories in the X - Y , X - Z and Y - Z planes drawn in Fig. 5a and the merged 3D image drawn in Fig. 5b clearly showed the 3D movement of the electric ray; however, it was difficult to know the speed of the ray at each point. Importantly, the speed is relative to the ray's motion state (swimming or stationary). This is indispensable information for seabed mapping. For mapping, position at the stationary state should be connected and the swimming state should be removed. On the other hand, it was easy to know when the ray was swimming or stationary from the displacement time-course trajectories of the electric ray plotted in Fig. 5c analyzed from the movie frames. When the ray was stationary, the line was flat. When the ray was

swimming, the line had a slope. By combining Fig. 5b,c, it was clearly shown that the ray was swimming in water or stationary at each point even without seeing the movies.

In this experiment, we demonstrated that the 3D movement of the benthic ray could be plotted on the XYZ coordinate system using the movies taken from 3 directions. Also, it was confirmed that the electric ray spent most of its time at the bottom. By connecting the points of the ray at the bottom which can be distinguished by the time courses of the movement, the 2D differences in height of the bottom would be known even if the geometry is unknown. Accordingly, we considered that the electric ray could be used for seabed mapping.

3.3 Seabed search using electric rays with pingers

Following the 3 fundamental experiments described above, we next demonstrated an actual seabed search using electric rays as shown in the concept of Fig. 6a. We carried out the experiment for the sea bottom with about 20 m water depth from a publicly available sea map (Fig. 6b) [28]. The size of the fishing boat which carried 4 receivers for the pingers was 12 m long and 3 m wide.

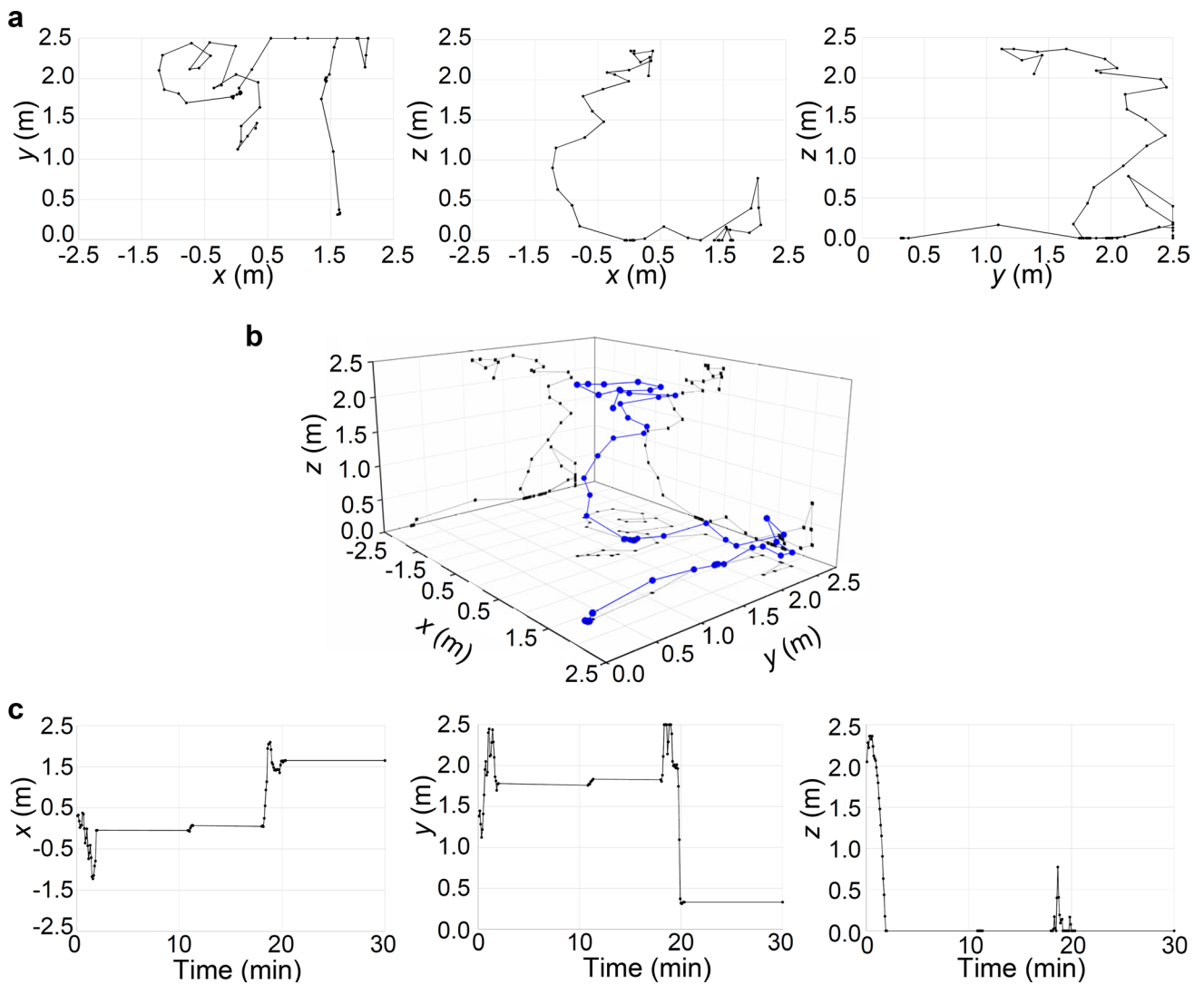


Fig. 5 Measurement results of the 3D movement of an electric ray in a water tank. **a** Plots of the movement of the ray on X–Y, Y–Z and X–Z plane per 5 s. **b** A 3D plot of the ray movement (30 min,

5 s interval). Blue points and line indicate 3D plots, and black points and line indicate projection in X–Y, X–Z, and Y–Z planes. **c** Time courses of the movement of x, y and z values of the ray

In this experiment, 2 electric rays equipped with small pingers were used. Each pinger (Fig. 6c) was connected to a security tag (Fig. 6d), and the pinger and tag were attached to each ray (Fig. 6e). Details for the attachment are described in Materials and methods. Acoustic signals were generated from the pingers regularly per second. The 4 receivers used these signals to identify the positions of the electric rays. The electric rays were connected to fishing lines coming from the fishing boat to avoid escaping from the measurable area (about 40 m from the boat). The two rays with attached pingers were put into the sea as shown in Fig. 6f. A control pinger attached to a weight was also lowered into the sea simultaneously. The role of the control pinger was to show that the electric rays actually moved in the bottom of the sea. It can be proved if the

movement of the control pinger due to the vibration of the ship was smaller than that for electric rays.

Data collected during the whole measurement period from when the electric rays were put into the sea to the time they were recovered after about 2 h are shown in Supplementary Figs. S2 and S3. The control pinger did not move significantly but laid on the sea bottom. On the other hand, it was difficult to fully trace movement of the pingers on the rays because the electric rays were sometimes pulled back to the boat to confirm they were still living. Therefore, the time period during which the rays were on or near the bottom was distinguished from the whole time course shown in Supplementary Fig. S4 and the corresponding data were extracted and re-plotted in Fig. 7a–d. Note that the data apparently during the pulled

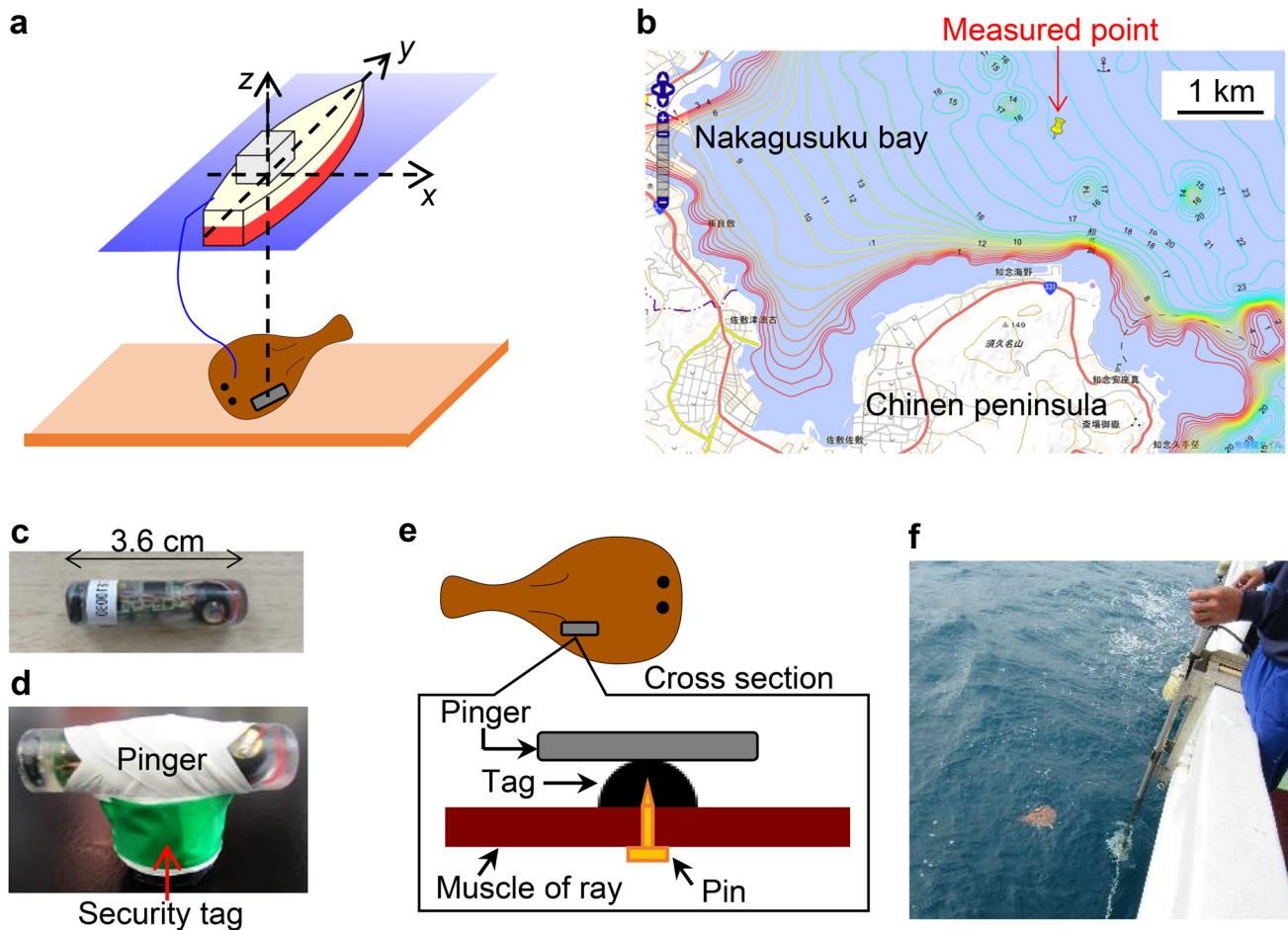


Fig. 6 Setup for measurement of the 3D movement of an electric ray in the sea when connected to a fishing boat. **a** Method using a pinger attached on the ray. Fishing line was connected between the ray and the boat to prevent the ray from leaving the study area. **b** Map showing the area used for this experiment. The area was near Nanjo City, Okinawa Prefecture, Japan. This map was cited from *Minnano Kaizu*. Longitude and latitude: 26°12' 23" N, 127° 49'

0" E. **c** Photograph of the pinger used for the experiment. **d** Photograph showing the pinger attached to a security tag by using glue and a tape. **e** Schematic showing the pinger and tag attached to the electric ray with a pin. **f** Photograph of an electric ray with the attached fishing line right after the ray was put into the sea from the boat

back to the boat and just after re-throwing were removed. From these 3D graphs, it was clear that the movements of the electric rays were much more active than the control pinger movement. The movements of the 2 electric rays were also different although they stayed in a similar area.

The displacement time-course trajectories for the control pingers and electric rays were also useful in this experiment to catch the timing of the movement of the rays. It is also clear that the movement of the control pinger was very small from start to finish (Supplementary Fig. S4). On the other hand, in case of electric ray #1 (Fig. 7e), there was a "jumping point" around $t=60$ min. At this timing, the x , y positions were suddenly changed, and the z position had a small peak. This phenomenon would indicate that the ray was swimming and moved dynamically at this time. Also, in the case of electric ray #2 (Fig. 7f), there was a jumping

point around $t=45$ min. In this case, the z position change was slight; however, there were gaps in x and y position traces, indicating that the ray moved around the bottom. There were no such jumping points in other time points, which meant that the electric rays were stationary or skimming or slipping slowly over the bottom surface in these periods. Importantly, these electric rays were active when they were pulled back to the boat and generated electricity even after finishing the experiments and having been in the sea for 2 h.

The existing map (Fig. 6b) was obtained using MBES which has high resolution under 1 m [10]. The vertical height difference between two successive contour lines in this sea map was 1 m. In the measurement area, the distance between the two successive contour lines was about 500 m. Since the maximum amplitude of the X–Y

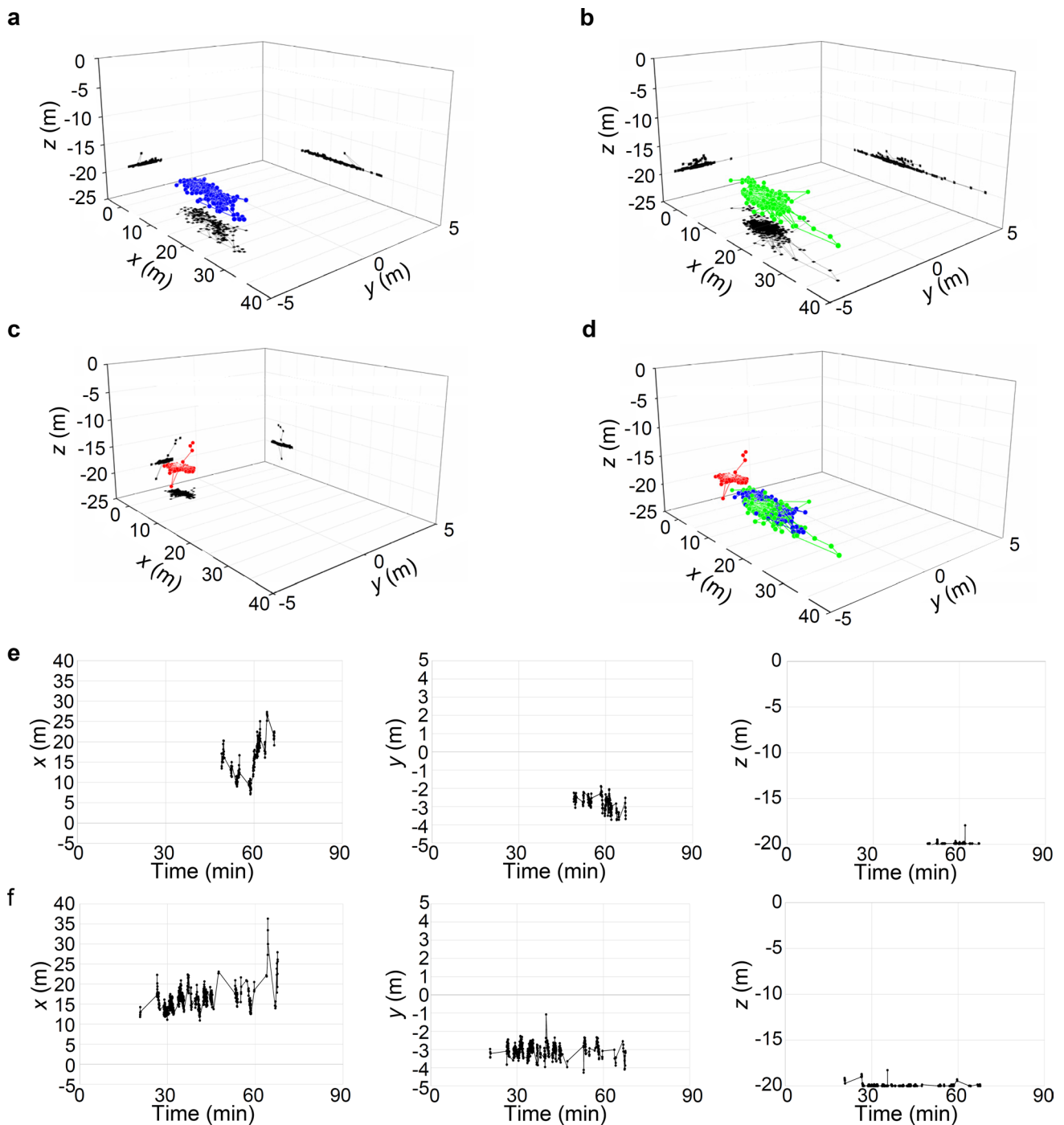


Fig. 7 Measurement result of the 3D movement of an electric ray in the sea when connected to a boat. **a**, **b** 3D plots of trajectories of the electric rays **a** #1 and **b** #2, while they were staying almost exclusively at the sea bottom. **c** 3D plots of trajectories of a control pinger with a weight for the whole time period. **d** A merged version

of the 3D plots of the 2 electric rays and the control pinger. Colored points and lines indicate 3D plots, and black points and line indicate projections in X-Y, X-Z, and Y-Z planes. **e**, **f** Time courses of the movements of x, y and z values of electric rays **e** #1 and **f** #2, while they were staying almost exclusively at the sea bottom

position of electric rays was about 40 m from Fig. 7, the average slope of this measurement area was within 0.1 m. The 0.10 m difference in height can be ignored because it is smaller than the vertical resolution of the depth

distribution measured by using a pinger. Moreover, the seabed in the nearby sea area was gentle as far as visual observations showed. Therefore, the sea bottom at the measured point was assumed to be flat which was similar

to the obtained data by using electric rays, even though a bathymetric map was not produced in this experiment.

From these results, the electric rays were confirmed to move around the sea bottom. This would be a spontaneous movement of the electric rays. Therefore, we found the possibility that terrain information of the sea can be mapped by the trajectories of the rays even though vibrations of the vessels should also be considered for precise measurement. Moreover, we confirmed that the electric rays were stationary or skimming or slipping slowly over the bottom surface most of the time which is typical benthic behavior required to search the seafloor depth distribution.

4 Discussion

We here compare the result with conventional, recent biotelemetry methods for biologging [29] as summarized in Table 1. This research proposes a new approach to explore physical information using biological behavior. This is completely different from conventional studies just exploring biological information using small communication devices (i.e., pingers). In addition, conventional studies fundamentally explore long-term behavior of fish for more than 1 day [30–33]. In these cases, rough positions and traces were usually tracked, but precise position time-course information was not obtained. There is a study capturing the precise movement track by using a high communication rate pinger, but it was not a benthic fish [34], or just using floating sensors which cannot provide terrain information [35]. On the other hand, our study revealed for the first time that the movement of benthic creatures can be traced nearly in real time.

We used sting and electric rays as an example of the benthic creatures. This method can be applied to other creatures as well. For instance, crabs are candidates for

seabed searching [36, 37]. But with most other creatures, the potential problem is the electricity supply. Energy harvesting methods must be developed to use other agents than electric rays.

The main advantage of our method is that it requires no external energy source for searching the seabed. This method can supply a new option for autonomous seabed mapping in addition to the data obtained by large-scale artificial systems including AUVs and sonar systems. For example, temporal changes of the seabed morphology could be monitored in addition to the acquisition of information about biota as discussed in Sect. 1. On the other hand, the disadvantage is that the precise control is difficult. Current method has 10 cm order resolution, but it includes some biological originated fluctuations. To compare the data with existing methods, such fluctuations must be removed by statistical or machine learning methods. By solving such issues, a seabed map will be created in the future.

Actually, a large number of rays are required to cover large areas. However, from the viewpoint of cost, rays are not expensive compared with ships or AUV. Although controllability is lower than those machines, self-regulation of creatures can reduce time by omitting complicated operations. Regarding ray numbers, more investigation will be required including the period to be used for searching, the area to be covered per ray in this period. Based on such data, the ray number will be estimated. Training the rays would be also a further future issue. Currently, we think to exploit just spontaneous behavior on the seabed.

The behavior of rays might be different compared to the natural condition when rays are in a water tank or connected by a line to a ship. However, the important point in this study is that we can distinguish whether rays are in the bottom or swimming in water from the moving speed of the rays. In this viewpoint, the behavior of the rays is the same in the two independent conditions (without a fish line in a water tank, and with a fish line, pinger in the sea). So, if focusing on this point, the behavior is expected to be the same in the natural condition.

Although the seabed used this time is flat, but we think that the principal purpose of this study is to confirm that the electric ray's position can be traced by pingers, and that the rays spent most of its time at the bottom as a first step of the mapping. This purpose was achieved this time. Creating a georeferenced seabed map with the depth distribution will be the next step. For checking the accuracy, comparison with conventional methods using sonar systems is required.

From the viewpoint of animal welfare, this method that exploits creatures might have a problem in the short term. To avoid invasion for animals, the use of miniaturized or flexible devices [38–40] which are also wearable

Table 1 Comparison of biotelemetry methods for various species

Species	References	Plotting time interval	Terrain information	Electric generation
Electric ray	This study	1 s	○	○
Antarctic fish	[30]	1 day	×	×
Finless porpoises	[31]	5 days	×	×
Shark	[32]	10 s	×	×
Seal	[33]	6 h	×	×
Tuna	[34]	0.05 s	×	×
Sting ray	[35]	5 min	×	×
Crab	[36]	1 s	○	×
Blue crab	[37]	10 min	○	×

or implantable for controlling the stimulation, sensing the behavior and saving the power of animals as well as avoiding long-term experiments would be necessary. However, from the long-term perspective, biota information including feed or natural enemies present in the area will be obtained. Such information would be useful to understand the fish number in the area and thus to avoid overfishing and animal welfare through conservation of the marine environment.

5 Conclusion

In this study, we used a large water tank (10 m × 5 m × 6 m height) to measure the movement patterns of benthic rays and confirmed that the speed of the sting and electric rays indicated whether they were skimming slowly over the bottom surface or swimming. Then, we equipped a small pinger on an electric ray and confirmed tracing of the movements of the rays over the sea bottom for more than 90 min at 1 s time resolution.

We confirmed typical benthic behavior of sting and electric rays required to search the seafloor depth distribution. By using either of sting or electric rays, the experiments would be carried out in all seasons. Although the sample size should be increased to precisely understand the behavior of the sting and electric rays, their fundamental behavior could be clarified. This is the minimum requirement for seabed mapping. However, to exploit the full, unique properties of electric rays for seabed searching, realizing the ways to save and use of electricity of the rays and investigation of biological properties of rays for obtaining biota information (feed or natural enemies present in the area) will be the extra issues to overcome.

Pingers that can be used in deep-sea areas below 5000 m are available [41]. Therefore, for deep-sea mapping which has been difficult to do by conventional methods, in the future, it would be possible to use this method with deep-sea creatures. For actual usage, we have to think about focusing the important area to be used for this method or increasing the deep-sea creatures.

Acknowledgements This work was funded by Grants-in-Aid for Scientific Research for Challenging Research (Exploratory) (18K18792) and Scientific Research on Innovative Areas (19H05338) from the Japan Society for the Promotion of Science (JSPS), Japan. This work was also financially supported by NIPPON Foundation, Japan Advanced Science and Technology Organization for education, human resource and research (JASTO) and Leave a Nest Co., Ltd., Japan, as part of the DeSET project promoted by them. We also thank Prof. K. Miyashita in Hokkaido University, Japan, and Dr. K. Minami in Shimane University, Japan, and Ms. A. Sato, RIKEN, Japan, for their technical advice and support.

Authors' contribution SF, NT and YT designed the research; SF, NT, SA, TS and YT conducted the research; AH and TS provide knowledge on the sea mapping; all authors interpreted the results; and SF, NT, SA and YT prepared the manuscript.

Compliance with ethical standards

Competing interests The authors declare no competing financial or non-financial interests.

Open Access This article is licensed under a Creative Commons Attribution 4.0 International License, which permits use, sharing, adaptation, distribution and reproduction in any medium or format, as long as you give appropriate credit to the original author(s) and the source, provide a link to the Creative Commons licence, and indicate if changes were made. The images or other third party material in this article are included in the article's Creative Commons licence, unless indicated otherwise in a credit line to the material. If material is not included in the article's Creative Commons licence and your intended use is not permitted by statutory regulation or exceeds the permitted use, you will need to obtain permission directly from the copyright holder. To view a copy of this licence, visit <http://creativecommons.org/licenses/by/4.0/>.

References

- Mayer L, Jakobsson M, Allen G, Dorschel B, Falconer R, Ferrini V, Lamarche G, Snaith H, Weatherall P (2018) The Nippon Foundation—GEBCO seabed 2030 project: the quest to see the world's oceans completely mapped by 2030. *Geosci* 8:63
- Thorsnes T, Bjarnadóttir LR, Jarna A, Baeten N, Scott G, Guinan J, Monteys X, Dove D, Green S, Gafeira J, Stevenson A (2018) National programmes: geomorphological mapping at multiple scales for multiple purposes. In: Micallef A, Krastel S, Savini A (eds) *Submarine geomorphology*. Springer, Cham, pp 535–552
- Li D, Wang P, Du L (2019) Path planning technologies for autonomous underwater vehicles: a review. *IEEE Access* 7:9745–9768
- Wynn RB, Huvenne VAI, Le Bas TP, Murton BJ, Connelly DP, Bett BJ, Ruhl HA, Morris KJ, Peakall J, Parsons DR, Sumner EJ, Darby SE, Dorrell RM, Hunt JE (2014) Autonomous underwater vehicles (AUVs): their past, present and future contributions to the advancement of marine geoscience. *Mar Geol* 352:451–468
- Sahoo A, Dwivedy SK, Robi PS (2019) Advancements in the field of autonomous underwater vehicle. *Ocean Eng* 181:145–160
- Cho H, Yu SC (2015) Real-time sonar image enhancement for AUV-based acoustic vision. *Ocean Eng* 104:568–579
- Yu SC, Teng Z, Kang DJ (2012) Modeling of high-resolution 3D sonar for image recognition. *Int J Offsh Pol Eng* 22:186–192
- Kang M, Nakamura T, Hamano A (2011) A methodology for acoustic and geospatial analysis of diverse artificial-reef datasets. *ICES J Mar Sci* 68:2210–2221
- Komatsu T, Igarashi C, Tatsukawa K, Sultana S, Matsuoka Y, Harada S (2003) Use of multi-beam sonar to map seagrass beds in Otsuchi Bay, on the Sanriku Coast of Japan. *Aquat Living Resour* 16:223–230
- Conti LA, Lim A, Wheeler AJ (2019) High resolution mapping of a cold water coral mound. *Sci Rep* 9:1016
- Diesing M, Stephens D (2015) A multi-model ensemble approach to seabed mapping. *J Sea Res* 100:62–69
- Janowski L, Tegowski J, Nowak J (2018) Seafloor mapping based on multibeam echosounder bathymetry and backscatter data

- using object-based image analysis: a case study from the Rewal site, the Southern Baltic. *Oceanol Hydrobiol St* 47:248–259
13. Prampolini M, Blondel P, Foglini F, Madricardo F (2018) Habitat mapping of the Maltese continental shelf using acoustic textures and bathymetric analyses. *Estuar Coast Shelf Sci* 207:483–498
 14. Sagawa T, Yamashita Y, Okumura T, Yamanokuchi T (2019) Satellite derived bathymetry using machine learning and multi-temporal satellite images. *Remote Sens* 11:1155
 15. Smith WHF, Sandwell DT (2019) Conventional bathymetry, bathymetry from space, and geodetic altimetry. *Oceanography* 17:8–23
 16. Dickey T, Lewis M, Chang G (2006) Optical oceanography: recent advances and future directions using global remote sensing and in situ observations. *Rev Geophys* 44:RG1001
 17. Irish JL, Lillycrop WJ (1999) Scanning laser mapping of the coastal zone: the SHOALS system. *ISPRS J Photogram* 54:123–129
 18. Gaitan-Espitia JD, Solano-Iguaran JJ, Tejada-Martinez D, Quintero-Galvis JF (2016) Mitogenomics of electric rays: evolutionary considerations within Torpediniformes (Batoidea; Chondrichthyes). *Zool J Linn Soc* 178:257–266
 19. Bray RN, Hixon MA (1978) Night-shocker: predatory behavior of the pacific electric ray (*Torpedo californica*). *Science* 200:333–334
 20. Lowe CG, Bray RN, Nelson DR (1994) Feeding and associated electrical behavior of the Pacific electric ray *Torpedo californica* in the field. *Mar Biol* 120:161–169
 21. Tanaka Y, Funano S, Nishizawa Y, Kamamichi N, Nishinaka M, Kitamori T (2016) An electric generator using living *Torpedo* electric organs controlled by fluid pressure-based alternative nervous systems. *Sci Rep* 6:25899
 22. Voegeli FA, Lacroix GL, Anderson JM (1998) Development of miniature pingers for tracking Atlantic salmon smolts at sea. *Hydrobiologia* 371(372):35–46
 23. Tang Y, Lin D, Zhang G, Zhang Z, Sasakura T (2013) Testing the tracking of behaviour of a caged Takifugu rubripes (Temminck & Schlegel, 1850) using acoustic telemetry. *J Appl Ichthyol* 29:1456–1458
 24. Sasakura T (2016) Underwater biotelemetry. *J Acoust Soc Jpn (in Japanese)* 72:207–211
 25. Miyoshi K, Kuwahara Y, Miyashita K (2018) Tracking the Northern Pacific sea star *Asterias amurensis* with acoustic transmitters in the scallop mariculture field of Hokkaido, Japan. *Fish Sci* 84:349–355
 26. Dean MN, Motta PJ (2004) Feeding behavior and kinematics of the lesser electric ray, *Narcine brasiliensis* (Elasmobranchii: Batoidea). *Zoology* 107:171–189
 27. Wilga CD, Maia A, Nauwelaerts S, Lauder GV (2012) Prey handling using whole-body fluid dynamics in batoids. *Zoology* 115:47–57
 28. A website providing seabed maps: *Minnano Kaizu* (2018) Retrieved from <https://mar-nets.com/> (in Japanese)
 29. Brooks JL, Chapman JM, Barkley AN, Kessel ST, Hussey NE, Hinch SG, Patterson DA, Hedges KJ, Cooke SJ, Fisk AT, Gruber SH, Nguyen VM (2019) Biotelemetry informing management: case studies exploring successful integration of biotelemetry data into fisheries and habitat management. *Can J Fish Aquat Sci* 76:1238–1252
 30. Miyamoto Y, Tanimura A (1999) Behavior of the Antarctic fish *Trematomus Bernacchii* (pisces, nototheniidae) beneath the sea ice near the Antarctic station Syowa using acoustic biotelemetry. *Fish Sci* 65:315–316
 31. Amano M, Kusumoto M, Abe M, Akamatsu T (2017) Long-term effectiveness of pingers on a small population of finless porpoises in Japan. *Endang Species Res* 32:35–40
 32. Voegeli FA, Smale MJ, Webber DM, Andrade Y, O'Dor RK (2001) Ultrasonic telemetry, tracking and automated monitoring technology for sharks. *Environ Biol Fish* 60:267–281
 33. McClintock BT, London JM, Cameron MF, Boveng PL (2017) Bridging the gaps in animal movement: hidden behaviors and ecological relationships revealed by integrated data streams. *Ecosphere* 8:e01751
 34. Hamano A, Sasakura T, Namari S, Sakakibara N, Ito S, Kodera K, Nomura T, Watanabe K, Nose M, Inai K, Nakamura T, Tanoue H (2018) Development of a new monitoring methodology for counting bluefin tuna in net pens. In: Proceedings of 2018 OCEANS-MTS/IEEE Kobe techno-oceans (OTO) conference and exhibition, 5p
 35. Martins APB, Heupel MR, Oakley-Cogan A, Chin A, Simpfendorfer CA (2020) Towed-float GPS telemetry: a tool to assess movement patterns and habitat use of juvenile stingrays. *Mar Freshw Res* 71:89–98
 36. Miyamoto Y, Uchida K, Orii R, Kakihara T, Furusawa M (2006) Validity of data filtering technique for the behavior analysis of crab in neritic and closed sea by ultrasonic biotelemetry. *Fish Sci* 72:211–213
 37. Bell GW, Eggleston DB, Wolcott TG (2003) Behavioral responses of free-ranging blue crabs to episodic hypoxia. II. Feeding. *Mar Ecol Prog Ser* 259:227–235
 38. Yalikul Y, Hosokawa Y, Iino T, Tanaka Y (2016) All-glass 12- μ m ultra-thin and flexible micro-fluidic chip fabricated by femto-second laser processing. *Lab Chip* 16:2427–2433
 39. Tanaka Y (2013) Electric actuating valves incorporated into an all glass-based microchip exploiting the flexibility of ultra thin glass. *RSC Adv* 3:10213–10220
 40. Sasaki N, Shinjo M, Hirakawa S, Nishinaka M, Tanaka Y, Mawatari K, Kitamori T, Sato K (2012) A palmtop-sized microfluidic cell culture system driven by a miniaturized infusion pump. *Electrophoresis* 33:1729–1735
 41. Edwards JE, Pratt J, Tress N, Hussey NE (2019) Thinking deeper: uncovering the mysteries of animal movement in the deep sea. *Deep-Sea Res Pt I* 146:24–43

Publisher's Note Springer Nature remains neutral with regard to jurisdictional claims in published maps and institutional affiliations.